Unfolding Kinetics of Human Telomeric G-Quadruplexes Studied by NMR Spectroscopy

ARTICLE *in* THE JOURNAL OF PHYSICAL CHEMISTRY B · JANUARY 2014

Impact Factor: 3.3 · DOI: 10.1021/jp410034d · Source: PubMed

THE JOURNAL OF PHYSICAL CHEMISTRY B

Article

pubs.acs.org/JPCB

Unfolding Kinetics of Human Telomeric G-Quadruplexes Studied by NMR Spectroscopy

Ming-Hao Li,[†,‡,#] Zi-Fu Wang,[†,§,#] Margaret Hsin-Jui Kuo,[†] Shang-Te Danny Hsu,*[,∥,⊥] and Ta-Chau Chang*[,†,‡,§]

[†]Institute of Atomic and Molecular Sciences, Academia Sinica, Taipei 106, Taiwan, R.O.C.

[‡]Institute of Biophotonics, National Yang-Ming University, Taipei 106, Taiwan, R.O.C.

[§]Department of Chemistry, National Taiwan University, Taipei 106, Taiwan, R.O.C.

[∥]Institute of Biological Chemistry, Academia Sinica, Taipei 115, Taiwan, R.O.C.

[⊥]Department of Biochemical Sciences, National Taiwan University, Taipei 106, Taiwan, R.O.C.

Supporting Information

ABSTRACT: Characterization of the unfolding kinetics of G-quadruplexes (G4s) is the key to a better understanding of the biological function of G4s and is important for biomedical research and material design. Of interest is that slight variations of human telomeric sequences can form different types of G4 structures. In general, there is a correlation between unfolding kinetics and thermal stability. Here we examined this correlation by first systematic analysis of the unfolding kinetics of a variety of telomeric G4 structures using the real-time imino proton NMR spectra of DNA hybridization and hydrogen−deuterium exchange (HDX). We then measured the melting temperature (T_m) and determined the Gibbs free energy (ΔG) of these G4 structures using differential scanning calorimetry (DSC). Our results showed that both T_m and ΔG are slightly structure-dependent, except the T_m of the parallel G4 structure is ∼10 °C higher than that of nonparallel G4 structures. The hybridization results showed that the decay times of different imino proton signals for each telomeric G4 structure are quite similar, which are also consistent with the time constant of the central G-tetrad obtained from HDX measurements. It is suggested that global unfolding is the rate-determining step for HDX, and each real-time imino proton NMR measurement can provide the intrinsic unfolding rate constant. The key finding is that the unfolding times of these various G4 structures are quite different and show no correlation between thermal stability and unfolding kinetics. Our results raised an issue that the folding and unfolding kinetics is more relevant for better understanding of biological function of G4 structures.

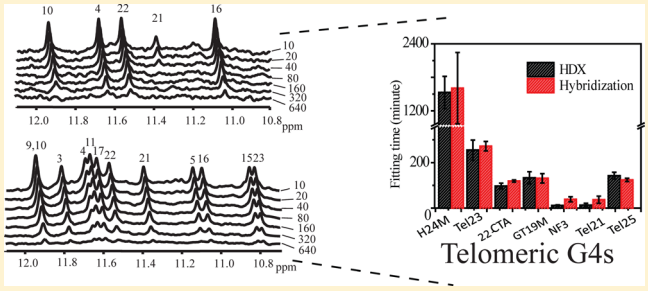

INTRODUCTION

Telomeres play a vital role in protecting the ends of eukaryotic chromosomes and preventing chromosomal fusion.[1,2] Telomeres contain 100−200 nt hexameric repeats of TTAGGG single-stranded sequence in the 3′-overhang, which can adopt an intramolecular G-quadruplex (G4) structure under physiological conditions *in vitro*,[3,4] in the meta-phase chromosome,[5] and *in vivo*.[6−8] G4s have recently emerged as a new class of molecular targets for anticancer drugs. While structural characterizations of a variety of G4 forming sequences have highlighted the structural polymorphism of G4s, rendering them challenging targets for structure-based drug design,[9,10] several small molecules have been developed to target G4s. Their abilities to modulate the folding stability of the target G4s have shown to be associated with altered gene transcription or translation;[11−14] therefore, it is of biomedical relevance to understand the structural stability and folding kinetics.[15] Indeed, one of the primary challenges in the field of biophysical studies in telomeric G4s is the structural polymorphism, which is directly associated with folding dynamics and kinetics. For example, NMR analysis showed that the human telomeric sequence, d[$AG_3(T_2AG_3)_3$] (Tel22), forms a basket antiparallel G4 structure in Na^+ solution,[16] while X-ray crystallography showed that Tel22 forms a propeller parallel G4 structure in the presence of K^+ condition.[17] In addition, NMR analyses showed that d[$TAG_3(T_2AG_3)_3$] (Tel23)[18] and d-[$TAG_3(T_2AG_3)_3TT$] (Tel25)[19] sequences adopt the (3 + 1) hybrid form I and II conformations in K^+ solution, respectively. Furthermore, d[$G_3(T_2AG_3)_3T$] (NF3), which differs in a single thymine residue at the 3′ end compared to Tel23 and Tel25, forms a basket antiparallel G4 structure with only two G-quartet layers in K^+ solution.[20] These examples illustrate that a small variation in human telomeric sequences can lead to profound differences in the G4 folding topologies.

Received: October 9, 2013
Revised: December 16, 2013
Published: January 9, 2014

   dx.doi.org/10.1021/jp410034d | *J. Phys. Chem. B* 2014, 118, 931−936

Table 1. Sequences of Different Telomeric G4s, Decay Time Constants of HDX, and Hybridaztion for Different G4s[a]

	sequence	topology	t_{HDX} (min)	t_{Hybrid} (min)
Tel23	$d[TAG_3(T_2AG_3)_3]$	(3 + 1) hybrid form-I	255 ± 43	273 ± 21
22-CTA	$d[AG_3(CTAG_3)_3]$	antiparallel chair form	97 ± 13	119 ± 5
GT19M	$d[(TAG_3)_2TG_3TAG_3]$	parallel propeller form	134 ± 27	131 ± 21
H24M	$d[TTG_3(T_2AG_3)_3A]$	(3 + 1) hybrid form-I	1530 ± 287	1606 ± 639
Tel25	$d[TAG_3(T_2AG_3)_3TT]$	(3 + 1) hybrid form-II	142 ± 15	124 ± 7
Tel21	$d[G_3(T_2AG_3)_3]$	n.d.	12 ± 3	36 ± 16
NF3	$d[G_3(T_2AG_3)_3T]$	antiparallel basket form	13 ± 8	39 ± 11

[a]sequence: sequences of different telomeric G4s. topology: topology of different G4 sequences. t_{HDX}: decay time constants of HDX experiment. t_{Hybrid}: decay time constants of hybridaztion experiment.

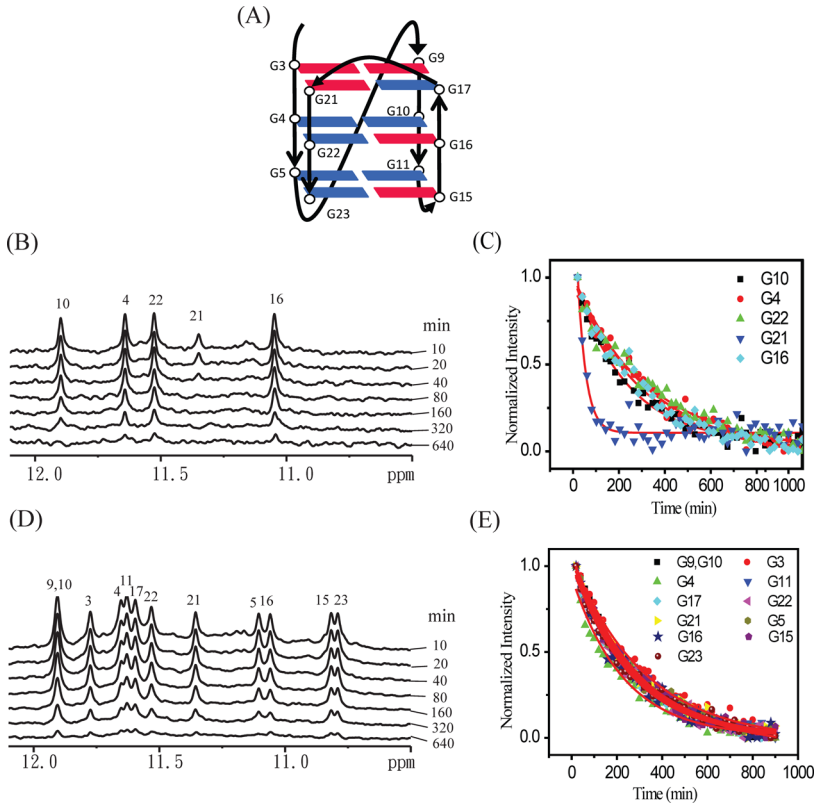

Figure 1. NMR HDX and hybridization experiments at 25 °C of Tel23. The structure of Tel23 with annotated nucleotides (A). Time-resolved imino proton spectra of Tel23 recorded at 10, 20, 40, 80, 160, 320, and 640 min after the addition of 99% D_2O (B) and complementary strand, C23 (D). The normalized peak intensities as a function of time in HDX (C) and hybridization (E) experiments. The data are fitted to a single exponential decay function (red line) to extract the corresponding decay time constant.

Several biophysical techniques can be used to study the thermodynamic and folding stabilities of G4s. For example, circular dichroism (CD) and UV absorption spectroscopy are common tools used to obtain the melting temperature (T_m) of G4s,[21,22] and calorimetric methods such as differential scanning calorimetry (DSC) can be used to extract enthalpy and heat capacity.[23−26] There are, however, limited reports on the folding kinetics of G4,[27,28] which evidently plays an integral part in the regulations of biological activities of G4s. NMR hydrogen−deuterium exchange (HDX) experiments afford unique insights into the folding events at the level of individual hydrogen bonds and thus thermodynamics as well as kinetics of the associated folding events can be extracted.[29] While NMR HDX has been widely used in the studies of protein folding[29−32] and DNA base pair stability,[33,34] it is under-represented in G4 folding studies.[35−37] In this work, we systematically investigate the folding of a variety of human telomeric G4s by NMR HDX and complementary strand hybridization experiments. Our results indicate that the thermal stabilities of G4s do not correlate with their folding kinetics; i.e., those that exhibit high melting temperatures do not necessarily unfold more slowly. These findings therefore warrant the need for further biophysical studies on the folding dynamics and kinetics of G4s in order to better understand the mechanism by which G4-forming sequences attain specific three-dimensional structures and the origin of their structural polymorphism.

MATERIALS AND METHODS

DNA Preparation. All oligonucleotides were purchased from Bio Basic (Ontario, Canada). The DNA concentrations were determined by the absorption at 260 nm peaks using a UV−vis absorption spectrometer (Nanoviewer, GE Healthcare, USA). The oligonucleotides were dissolved in 10 mM Tris−

dx.doi.org/10.1021/jp410034d | J. Phys. Chem. B 2014, 118, 931−936

HCl (pH 7.5) and 150 mM K^+, followed by heat-denaturation at 95 °C for 5 min, and slow annealing to room temperature (1 °C/min). The annealed oligonucleotides were stored at 4 °C before experiments.

NMR Kinetic Measurements. All NMR experiments were performed on Bruker AVIII 500 MHz and AVIII 800 MHz spectrometers (Bruker, Germany), which are equipped with a prodigy or a cryo-probe at 25 °C, respectively. One dimension (1D) imino proton NMR spectra were recorded using a WATERGATE pulsed sequence or a jump-and-return (JR) scheme for solvent suppression. The G4 oligonucleotides for the HDX exchange experiments were buffered in 150 mM K^+, 10 mM Tris−HCl (pH 7.5), followed by an annealing procedure as described above, and then lyophilized. The lyophilized oligonucleotides were resuspended in D_2O (99%) immediately before NMR measurements to reach a DNA concentration of 100 μM. For the hybridization experiments, the G4 and its complementary strand were buffered in 150 mM K^+, with a strand concentration of 200 μM. The experiment was performed by mixing a complementary strand sample into an equal amount of a G4 sample. All data are processed by Topspin 2.1 (Bruker, Germany) and analyzed by Origin 8.5 (OriginLab, USA).

Differential Scanning Calorimetry (DSC). DSC thermograms were measured using an N-DSC III calorimeter (New Castle, DE, USA). The data acquisition and analysis were carried out using the built-in software (NanoDSC Run version 3.6 and NanoAnalyze version 2.0). Each calorimetric experiment of 200 μM was performed by scanning from the sample from 20 to 110 °C at 1.0 °C/min. The corresponding baseline (buffer−buffer) scans were subtracted from the buffer−sample scans before their normalization and analysis.

RESULTS

Unfolding Kinetics of G4 Structure by NMR HDX Experiment. NMR HDX has been used to study the folding kinetics of G4s.[35−37] The rates of HDX report on the dynamics of hydrogen bonds within the G-tetrads at a resolution of individual guanines.[35−37] The HDX rates reflect the folding stability and extent of solvent exposure of the hydrogen bond donors.[35−38] The slower they are, the more protected the hydrogen bond donors, i.e., imino groups of G-tetrads, are. The rates of HDX also reflect the degree of local fluctuations of individual Hoogsteen hydrogen bonds within the G4 structure. In most cases, the imino protons in the top and bottom G-tetrads exchange much faster than those within the middle layer G-tetrad that is sandwiched by the top and bottom layers. NMR HDX is therefore commonly used to verify the most protected imino protons, usually the four in the central G-tetrads of G4 structure with similar degrees of protection with the time scale of HDX typically in hours. We set out to employ NMR HDX experiment to investigate the unfolding kinetics of several G4s (Table 1) of which the solution structures have been determined by NMR spectroscopy, and hence, their imino proton chemical shifts are readily available for residue-specific analyses.

Our first model system is Tel23 G4 (Figure 1A). Immediately after dissolving the K^+ form of Tel23 G4 in D_2O buffer, only five imino proton resonances remain, four of which correspond to the four guanines in the central G-tetrad, namely, G4, G10, G16, and G22 with a similar HDX time constant of ca. 255 ± 43 min, and the fifth one corresponds to the imino proton of G21 (37 ± 7 min, Table S1, Supporting Information), which exchanges much more rapidly than those in the central G-tetrad[18] (Figure 1B,C). The slower HDX rate of G21 is likely due to the additional protection from the loop that sequesters the imino proton of G21 from solvent exposure, as seen in the reported structure (PDB entry 2DL8).[18] Similarly, kinetics of other G4s are examined by HDX experiment (Figure S1 and Table S1, Supporting Information). The decay times of the imino proton signals from HDX experiment are 97 ± 13 min for 22-CTA, 134 ± 27 min for GT19M, 1530 ± 287 min for H24M, 142 ± 15 min for Tel25, 12 ± 3 min for Tel21, and 13 ± 8 min for NF3 (Table 1). Thus, HDX can provide structural information for G4 with a specific topology or flanking group.

Unfolding Kinetics of G4 Structure by Hybridization NMR Experiment. To complement the information extracted from the HDX experiments, we carry out hybridization experiments to observe the unfolding of the G4s by monitoring the loss of G4 imino proton resonances upon the addition of antisense strands that will hybridize with the G4 sequences to form duplex structures. The formation of a DNA duplex will result in downfield shifts of the imino protons from 11 to 12 to 13−14 ppm, which corresponds to a change of Hoogsteen base-pairing into Watson−Crick base-pairing.[39−42] By fitting the time-resolved signals of G4 imino protons to a single exponential decaying function, the unfolding kinetics of the G4 structure can be obtained with the assumption of the antisense strand acting as bait without perturbing the unfolding kinetics of G4. Figure 1D shows that, upon the addition of the antisense sequence C23 (d[$(CCCTAA)_3$CCCTA]) to Tel23 G4, the intensities of the imino protons decay at approximately the same rate, with a time constant of 273 ± 21 min (Figure 1E). This suggests that the hybridization is probing the global unfolding events. Furthermore, the average hybridization time constant is very similar to the average HDX time constant of the central G-tetrad (Table 1), which further confirms that the global unfolding is the rate-limiting step for HDX and hence the HDX time constants reported on the unfolding kinetics correspond to the EX1 regime for HDX;[28−31] i.e., the system is not in equilibrium but rather limited by the opening of the hydrogen bond of interest.

We apply the same hybridization analysis to other G4s to examine whether their unfolding kinetics is similar to that of Tel23 G4 (Figure S2 and Table S2, Supporting Information). Similar to Tel23, the hybridization time constants of the three-layer G4s are similar to their respective HDX time constants (Table 1). We can therefore conclude that, for all the three-layer G4s that we have examined herein, the HDX of the central G-tetrads is kinetically controlled by the global unfolding, which is confirmed by the hybridization experiments. However, for NF3, which forms the basket-type G4 topology with only two G-quartet layers without a central G-tetrad to be sandwiched by two other G-tetrads, the HDX time constants are much shorter than those determined by hybridization experiments, an observation attributed to the dominating contributions from local fluctuations in HDX,[35−37] which are much faster than global unfolding.

Collectively, we have obtained a linear relationship shown between time constants of HDX and hybridization (Figure 2) (R^2 = 0.97 with a slope of 1.05). With the exception of the two-layered NF3, the HDX of G4s reported on the global unfolding of G4 structures is consistent with the results obtained from complementary strand hybridization.

dx.doi.org/10.1021/jp410034d | J. Phys. Chem. B 2014, 118, 931−936

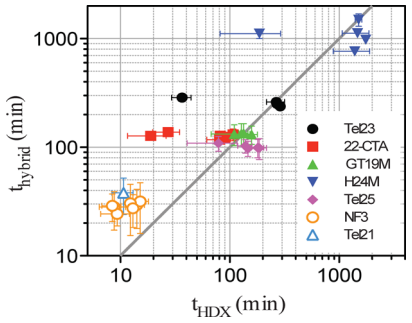

Figure 2. The correlation plot between the decay time constants of HDX and those of hybridization for different G4s. The gray line shows the boundary where the two decay time constants are equal. For Tel23, 22-CTA, and H24M, the outliers correspond to the imino protons that are located at the top or bottom layer, which display shorter HDX time constants due to local fluctuations. The HDX time constants of NF3 and Tel21 are systematically shorter than their hybridization time constants.

Thermal and Kinetics Stability of Different G4 Structures. Having established the unfolding kinetics of a variety of G4 structures, we next examine whether those G4s that exhibit slow unfolding kinetics are also thermodynamically more stable. Systematic surveys using spectroscopic methods have shown that the thermal stability of DNA G4s is associated with the lengths of the loops that connect individual G-tracts: the shorter the loop lengths are, the more thermally stable they are.[43,44] DSC is a powerful tool that can also be used to extract melting temperatures, unfolding enthalpies, and heat capacities under equilibrium conditions.[23−26] We have employed DSC to determine the melting temperature (T_m) and enthalpy (ΔH) associated with thermal unfolding for the G4s examined herein (Figure 3). All G4s exhibit monophasic transitions, and the T_m values range between 67 and 82 °C (Table S3, Supporting Information). The enthalpy (ΔH) is about ca. 50 kcal/mol for these G4s. The associated entropy (ΔS) can be calculated from

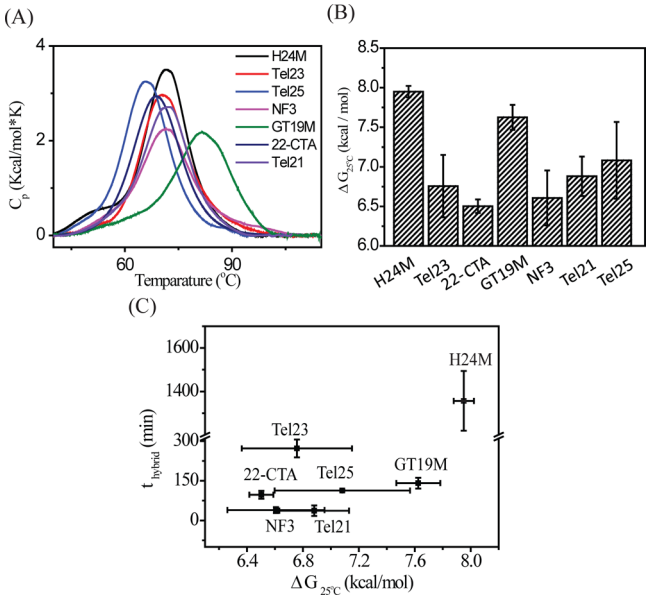

Figure 3. (A) DSC thermogram of G4s in 150 mM K^+ solution. (B) Calculated ΔG from DSC for G4s. (C) Time constant of hybridization (t_{hybrid}) vs ΔG for G4s.

T_m and ΔH, and the free energy of unfolding (ΔG) can then be obtained on the basis of the equation $\Delta G = \Delta H - T\Delta S$ (Table S3, Supporting Information). Among all the G4s, the parallel G4 topology (GT19M) is the most stable structure (Figure 3B). However, the unfolding kinetics of GT19M is significantly faster than that of Tel23, and moreover, the unfolding time constant of NF3, which contains only two layers of G-tetrads (Table 1), is the shortest despite the higher thermodynamic stability compared to some of the other G4s (Figure 3). Taken together, our results show that the thermal stability (free energy) of a given G4 does not necessarily correlate with its unfolding kinetics (unfolding time constant) (Figure 3C).

The equilibrium constant (K) of folding and unfolding can be extracted from DSC measurements as

$$\Delta G = -RT \ln K \quad (1)$$

and

$$K = k_f/k_u \quad (2)$$

where k_f is the folding rate constant and k_u is the unfolding rate constant. The unfolding rate constant, k_u, can be determined by NMR HDX and hybridization measurements ($k_u = 1/\tau_u$), where τ_u is the unfolding decay time. Therefore, the folding rate constant (k_f) can then be calculated using eq 2 (Table 2). The calculated results are in good agreement with previously reported values derived from stopped-flow kinetics measurement.[27,28]

Table 2. Kinetic Parameters of Various G4 Structures at 25 °C[a]

	GT19M	Tel23	22-CTA	Tel25	NF3	H24M
K (10^4) (DSC)	40.6	9.5	6.1	16.3	7.3	71.0
k_u (10^{-4} s^{-1})	1.25	0.63	1.54	1.25	4.27	0.12
τ_u (min)	133	264	108	133	39	1568
k_f (s^{-1})	50.8	5.97	9.39	0.4	31.3	7.55
τ_f (ms)	20	168	106	49	31	132

[a] K: equilibrium constant obtained from DSC. k_u: unfolding rate constant. τ_u: average unfolding time obtained from NMR HDX and hybridization experiment. k_f: calculated folding rate constant. τ_f: calculated folding time.

According to the relationship between DSC results and unfolding decay times, it appears that thermodynamic measurements cannot be used to distinguish the differences in G4 structural diversities, especially in different human telomeric G4s, which have merely few base differences in sequence compositions. As the equilibrium constant is directly related to folding and unfolding rate constants, the difference can be diminished by fluctuation of both folding and unfolding rate constants. Therefore, this is probably the reason for the lack of correlation between kinetic and thermodynamic stability.

Unfolding Kinetics Stability of Tel23 as a Function of K^+ Concentrations. Having established the thermal stabilities of a variety of G4s by DSC, we next ask the question of whether the unfolding kinetics of a given G4 is dependent on the concentration of potassium ion as is for the thermal stability. For Tel23, a strong correlation ($R^2 = 0.99$) exists between the free energy of unfolding and the unfolding time constant (as determined by NMR hybridization experiment) (Figure 4). While previous reports have indeed shown that high potassium concentrations have a stabilizing effect on the T_m of various G4s,[23−26] it is not trivial to conclude that the unfolding kinetics

dx.doi.org/10.1021/jp410034d | J. Phys. Chem. B 2014, 118, 931−936

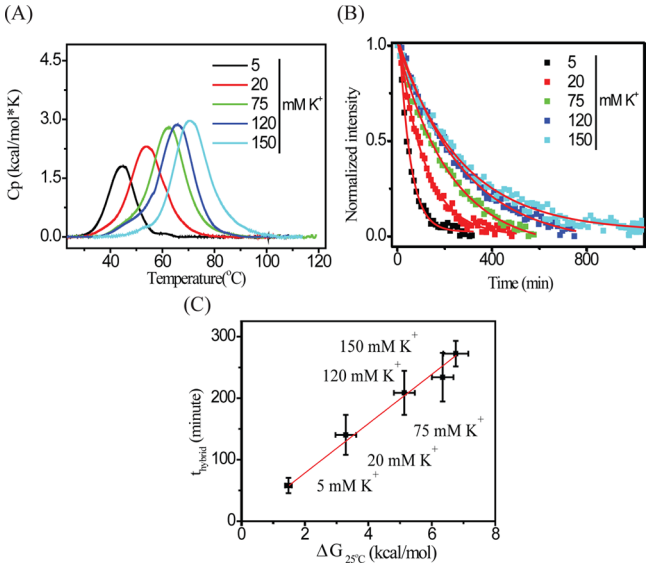

Figure 4. (A) DSC thermograms of Tel23 G4 at different K^+ concentrations. (B) Decay curves of the NMR imino proton signals of Tel23 upon adding equal amounts of antisense DNA at various K^+ concentrations. (C) A plot of ΔG vs unfolding time for Tel23 at various K^+ concentrations.

positively correlates with the thermal stability. In addition, a previous study has shown that the folding rate becomes more rapid as the K^+ concentration increases.[27,28] Therefore, our results provide the evidence that unfolding time increases as K^+ concentration increases, and suggest both folding and unfolding processes contribute positively to equilibrium constant with K^+ concentration effect.

CONCLUSION

In summary, our current results provide insights into the kinetic stability of various G4 structures, and highlight the discrepancy between their kinetic stability and thermodynamic stability. Finally, the strategy of NMR HDX and hybridization to approach intrinsic G4 unfolding time can be further explored to interaction of G4 structure with related ligand or protein.

ASSOCIATED CONTENT

Supporting Information

Spectra of NMR HDX and hybridization experiments for different G4s. Tables of the NMR HDX and hybridization decay time constants for individual guanine of various G4s. Thermodynamic parameters obtained from DSC. This material is available free of charge via the Internet at http://pubs.acs.org.

AUTHOR INFORMATION

Corresponding Authors

*E-mail: sthsu@gate.sinica.edu.tw.
*E-mail: tcchang@po.iams.sinica.edu.tw.

Author Contributions

#These authors contributed equally to this work.

Notes

The authors declare no competing financial interest.

ACKNOWLEDGMENTS

This work was supported by Academia Sinica (AS-102-TP-A07) and the National Science Council of the Republic of China (Grant NSC-101-2113-M001-022). S.-T.D.H. is a recipient of the Career Development Award (CDA - 00025/2010-C) from the International Human Frontier Science Program and is supported by funding from the National Science Council (100-2113-M-001-031-MY2 and 101-2627-M-001-004) and Academia Sinica, Taiwan. We thank Dr Shing-Jong Huang (Instrumentation Center, National Taiwan University) for assistance in obtaining the Bruker AVIII 500 and 800 MHz FT-NMR data and Dr. Chris Jao (Biophysical core facility, Academia Sinica) for her assistance on the DSC experiments.

REFERENCES

(1) Blackburn, E. H. Structure and Function of Telomeres. *Nature* **1991**, *350*, 569−573.
(2) Cech, T. R. Beginning to Understand the End of the Chromosome. *Cell* **2004**, *116* (2), 273−279.
(3) Williamson, J. R.; Raghuraman, M. K.; Cech, T. R. Monovalent Cation-Induced Structure of Telomeric DNA: the G-Quartet Model. *Cell* **1989**, *59*, 871−880.
(4) Sundquist, W. I.; Klug, A. Telomeric DNA Dimerizes by Formation of Guanine Tetrads between Hairpin Loops. *Nature* **1989**, *342*, 825−829.
(5) Chang, C. C.; Kuo, I. C.; Ling, I. F.; Chen, C. T.; Chen, H. C.; Lou, P. J.; Lin, J. J.; Chang, T. C. Detection of Quadruplex DNA Structures in Human Telomeres by a Fluorescent Carbazole Derivative. *Anal. Chem.* **2004**, *76*, 4490−4494.
(6) Biffi, G.; Tannahill, D.; McCafferty, J.; Balasubramanian, S. Quantitative Visualization of DNA G-Quadruplex Structures in Human Cells. *Nat. Chem.* **2013**, *5*, 182−186.
(7) Lam, E. Y.; Beraldi, D.; Tannahill, D.; Balasubramanian, S. G-Quadruplex Structures are Stable and Detectable in Human Genomic DNA. *Nat. Commun.* **2013**, *4*, 1796.
(8) Tseng, T. Y.; Wang, Z. F.; Chien, C. H.; Chang, T. C. In-Cell Optical Imaging of Exogenous G-Quadruplex DNA by Fluorogenic Ligands. *Nucleic Acids Res.* **2013**, *41*, 10605−10618.
(9) Patel, D. J.; Phan, A. T.; Kuryavyi, V. Human Telomere, Oncogenic Promoter and 5′-UTR G-Quadruplexes: Diverse Higher Order DNA and RNA Targets for Cancer Therapeutics. *Nucleic Acids Res.* **2007**, *35*, 7429−7255.
(10) Balasubramanian, S.; Neidle, S. G-quadruplex Nucleic Acids as Therapeutic Targets. *Curr. Opin. Chem. Biol.* **2009**, *13*, 345−353.
(11) Kumari, S.; Bugaut, A.; Huppert, J. L.; Balasubramanian, S. An RNA G-Quadruplex in the 5′ UTR of the *NRAS* Proto-Oncogene Modulates Translation. *Nat. Chem. Biol.* **2007**, *3*, 218−221.
(12) Rankin, S.; Reszka, A. P.; Huppert, J.; Zloh, M.; Parkinson, G. N.; Todd, A. K.; Ladame, S.; Balasubramanian, S.; Neidle, S. Putative DNA Quadruplex Formation within the Human *c-kit* Oncogene. *J. Am. Chem. Soc.* **2005**, *127*, 10584−10589.
(13) Siddiqui-Jain, A.; Grand, C. L.; Bearss, D. J.; Hurley, L. H. Direct Evidence for a G-Quadruplex in a Promoter Region and its Targeting with a Small Molecule to Repress c-MYC Transcription. *Proc. Natl. Acad. Sci. U.S.A.* **2002**, *99*, 11593−11598.
(14) Cogoi, S.; Xodo, L. E. G-quadruplex Formation within the Promoter of the *KRAS* Proto-Oncogene and its Effect on Transcription. *Nucleic Acids Res.* **2006**, *34*, 2536−2549.
(15) Lane, A. N.; Chaires, J. B.; Gray, R. D.; Trent, J. O. Stability and Kinetics of G-Quadruplex Structures. *Nucleic Acids Res.* **2008**, *36*, 5482−5515.
(16) Wang, Y.; Patel, D. J. Solution Structure of the Human Telomeric Repeat $d[AG_3(T_2AG_3)_3]$ G-tetraplex. *Structure* **1993**, *1*, 263−282.
(17) Parkinson, G. N.; Lee, M. P.; Neidle, S. Crystal Structure of Parallel Quadruplexes from Human Telomeric DNA. *Nature* **2002**, *417*, 876−880.
(18) Luu, K. N.; Phan, A. T.; Kuryavyi, V.; Lacroix, L.; Patel, D. J. Structure of the Human Telomere in K^+ Solution: an Intramolecular (3 + 1) G-Quadruplex Scaffold. *J. Am. Chem. Soc.* **2006**, *128*, 9963−9970.

(19) Phan, A. T.; Luu, K. N.; Patel, D. J. Different Loop Arrangements of Intramolecular Human Telomeric (3 + 1) G-Quadruplexes in K^+ Solution. *Nucleic Acids Res.* **2006**, *34*, 5715−5719.
(20) Lim, K. W.; Amrane, S.; Bouaziz, S.; Xu, W.; Mu, Y.; Patel, D. J.; Luu, K. N.; Phan, A. T. Structure of the Human Telomere in K^+ Solution: a Stable Basket-Type G-Quadruplex with Only Two G-Tetrad Layers. *J. Am. Chem. Soc.* **2009**, *131*, 4301−4309.
(21) Mergny, J. L.; Phan, A. T.; Lacroix, L. Following G-Quartet Formation by UV-Spectroscopy. *FEBS Lett.* **1998**, *435*, 74−78.
(22) Balagurumoorthy, P.; Brahmachari, S. K.; Mohanty, D.; Bansal, M.; Sasisekharan, V. Hairpin and Parallel Quartet Structures for Telomeric Sequences. *Nucleic Acids Res.* **1992**, *20*, 4061−4067.
(23) Petraccone, L.; Erra, E.; Nasti, L.; Galeone, A.; Randazzo, A.; Mayol, L.; Barone, G.; Giancola, C. Effect of a Modified Thymine on the Structure and Stability of $[d(TGGGT)]_4$ Quadruplex. *Int. J. Biol. Macromol.* **2003**, *31*, 131−137.
(24) Olsen, C. M.; Gmeiner, W. H.; Marky, L. A. Unfolding of G-quadruplexes: Energetic, and Ion and Water Contributions of G-Quartet Stacking. *J. Phys. Chem. B* **2006**, *110*, 6962−2969.
(25) Chaires, J. B. A Thermodynamic Signature for Drug-DNA Binding Mode. *Arch. Biochem. Biophys.* **2006**, *453*, 26−31.
(26) Lin, C. T.; Tseng, T. Y.; Wang, Z. F.; Chang, T. C. Structural Conversion of Intramolecular and Intermolecular G-Quadruplexes of bcl2mid: the Effect of Potassium Concentration and Ion Exchange. *J. Phys. Chem. B* **2011**, *115*, 2360−2370.
(27) Gray, R. D.; Chaires, J. B. Kinetics and Mechanism of K^+- and Na^+-Induced Folding of Models of Human Telomeric DNA into G-Quadruplex Structures. *Nucleic Acids Res.* **2008**, *36*, 4191−4203.
(28) Zhang, A. Y.; Balasubramanian, S. The Kinetics and Folding Pathways of Intramolecular G-Quadruplex Nucleic Acids. *J. Am. Chem. Soc.* **2012**, *134*, 19297−19308.
(29) Englander, S. W.; Kallenbach, N. R. Hydrogen Exchange and Structural Dynamics of Proteins and Nucleic Acids. *Q. Rev. Biophys.* **1983**, *16*, 521−655.
(30) Krishna, M. M.; Hoang, L.; Lin, Y.; Englander, S. W. Hydrogen Exchange Methods to Study Protein Folding. *Methods* **2004**, *34*, 51−64.
(31) Hsu, S.-T. D.; Blaser, G.; Behrens, C.; Cabrita, L. D.; Dobson, C. M.; Jackson, S. E. Folding Study of Venus Reveals a Strong Ion Dependence of its Yellow Fluorescence under Mildly Acidic Conditions. *J. Biol. Chem.* **2010**, *285*, 4859−4869.
(32) Andersson, F. I.; Werrell, E. F.; McMorran, L.; Crone, W. J. K.; Das, C.; Hsu, S.-T. D.; Jackson, S. E. The Effect of Parkinson's Disease Associated Mutations on the Deubiquitinating Enzyme UCH-L1. *J. Mol. Biol.* **2011**, *407*, 261−272.
(33) Steinert, H. S.; Rinnenthal, J.; Schwalbe, H. Individual Basepair Stability of DNA and RNA Studied by NMR-Detected Solvent Exchange. *Biophys. J.* **2012**, *102*, 2564−2574.
(34) Every, A. E.; Russu, I. M. Probing the Role of Hydrogen Bonds in the Stability of Base Pairs in Double-Helical DNA. *Biopolymers* **2007**, *87*, 165−173.
(35) Phan, A. T.; Modi, Y. S.; Patel, D. J. Propeller-Type Parallel-Stranded G-Quadruplexes in the Human *c-myc* Promoter. *J. Am. Chem. Soc.* **2004**, *126*, 8710−7816.
(36) Hsu, S. T.; Varnai, P.; Bugaut, A.; Reszka, A. P.; Neidle, S.; Balasubramanian, S. A G-Rich Sequence within the *c-kit* Oncogene Promoter Forms a Parallel G-Quadruplex Having Asymmetric G-Tetrad Dynamics. *J. Am. Chem. Soc.* **2009**, *131*, 13399−13409.
(37) Bugaut, A.; Rodriguez, R.; Kumari, S.; Hsu, S. T.; Balasubramanian, S. Small Molecule-Mediated Inhibition of Translation by Targeting a Native RNA G-Quadruplex. *Org. Biomol. Chem.* **2010**, *8*, 2771−2776.
(38) Zavasnik, J.; Podbevsek, P.; Plavec, J. Observation of Water Molecules within the Bimolecular $d(G_3CT_4G_3C)_2$ G-Quadruplex. *Biochemistry* **2011**, *50*, 4155−4161.
(39) Phan, A. T.; Mergny, J. L. Human Telomeric DNA: G-Quadruplex, i-Motif and Watson-Crick Double Helix. *Nucleic Acids Res.* **2002**, *30*, 4618−4625.
(40) Phan, A. T.; Patel, D. J. Two-Repeat Human Telomeric d(TAGGGTTAGGGT) Sequence Forms Interconverting Parallel and Antiparallel G-Quadruplexes in Solution: Distinct Topologies, Thermodynamic Properties, and Folding/Unfolding Kinetics. *J. Am. Chem. Soc.* **2003**, *125*, 15021−15027.
(41) Lane, A. N. The Stability of Intramolecular DNA G-Quadruplexes Compared with Other Macromolecules. *Biochimie* **2012**, *94*, 277−286.
(42) Adrian, M.; Heddi, B.; Phan, A. T. NMR Spectroscopy of G-Quadruplexes. *Methods* **2012**, *57*, 11−24.
(43) Risitano, A.; Fox, K. R. Influence of Loop Size on the Stability of Intramolecular DNA Quadruplexes. *Nucleic Acids Res.* **2004**, *32*, 2598−2606.
(44) Bugaut, A.; Balasubramanian, S. A Sequence-Independent Study of the Influence of Short Loop Lengths on the Stability and Topology of Intramolecular DNA G-Quadruplexes. *Biochemistry* **2008**, *47*, 689−697.